Contents lists available at ScienceDirect

Arabian Journal of Chemistry

journal homepage: www.ksu.edu.sa

Synthesis and evaluation of an environmentally friendly phosphorus-free and nitrogen-free polymer as a scale and corrosion inhibitor

Xinhua Liu [a,*], Yuhua Gao [b], Baojing Luo [a], Hongxia Zhang [a], Xiaoyu Shi [a,b], Yuan Zhang [a], Yongguang Gao [a], Ying Wang [a], Zilin Zheng [a], Nan Ma [a], Jiarui Du [a], Linyan Gu [a]

[a] Department of Chemistry, Tangshan Normal University, Tangshan 063000, Hebei, China
[b] Institute of Energy Resources, Hebei Academy of Sciences, Shijiazhuang 050081, Hebei, China

ARTICLE INFO

Keywords:
Green scale inhibitor
Green corrosion inhibitor
Modified polyepoxysuccinic acid
Interface protection

ABSTRACT

Polyepoxysuccinic acid (PESA) was modified by glycidyl (Gly) to obtain a phosphate-free and nitrogen-free polymer (Gly-PESA), and its scale and corrosion inhibition properties were studied.The effects of Gly-PESA concentration, calcium ion concentration and temperature to scale inhibition performance were studied by static scale inhibition method. The corrosion inhibition performance of Gly-PESA was studied by static weight-loss method. The morphology and structure of calcium scale and steel surface were characterized by spectroscopic and microscopic methods. The scale inhibition efficiency of Gly-PESA for $CaCO_3$ and $CaSO_4$ was 98.06% and 92.6%, respectively. Under the same experimental conditions, the scale inhibition effect of Gly-PESA was obviously better than that of PESA. Gly-PESA could effectively inhibit the growth of $CaCO_3$ and $CaSO_4$ crystals and cause their crystal lattice distortion or crystal dispersion. The corrosion inhibition efficiency of Gly-PESA for carbon steel was 78.17%. The adsorption of Gly-PESA on the surface of the steel test piece followed Langmuir adsorption isotherm, and formed a protective film, which increased the corrosion resistance of the steel test piece, thus effectively protecting the steel test piece. Therefore, Gly-PESA was a green scale and corrosion inhibitor, which solved the problem of environmental pollution.

1. Introduction

With the accelerated development of industrial production and the rapid increase in industrial water consumption, industrial cooling water accounted for more than 60 %–70 % of industrial water. Industrial cooling water could cause corrosion, scaling and microbial slime problems on the surface of equipment and pipes, thereby shortening the service life of equipment and pipes (Quraishi et al., 2010, Htet and Zeng, 2022,Touir et al., 2009). Mineral ions in industrial cooling water systems, such as bicarbonate ions and calcium ions, might settle on the surface of heat transfer equipment (such as heat exchangers, evaporators and condensers) to form scale. In addition, corrosion was also a major problem for cooling water systems, as the consequences of corrosion could lead to loss of reliability, process contamination, reduced system performance, increased maintenance costs, or unplanned downtime (Htet and Zeng, 2022, Yee et al., 2019). The two main operational problems of cooling water systems were corrosion and scaling due to electrochemical redox reactions and the deposition of metal salts on metal surfaces. Therefore, in order to solve these problems in cooling water systems, various inhibitors have been used (Htet and Zeng, 2022, Zeng and Qin, 2012, Sharma and Kumar, 2021).

In the era of world environmental protection laws and regulations, the concept of green chemistry and green water treatment agents has been deeply rooted in people's hearts (Liu et al., 2014). Traditional and natural scale and corrosion inhibitors had problems such as high operating cost and large drug dosage. In addition, corrosion inhibitors and scale inhibitors containing phosphorus had poor scale inhibition effect on calcium phosphate, zinc scale and iron oxide precipitation or caused changes in water quality. At present, PESA and polyaspartic acid (PASP) were identified as scale and corrosion inhibitors for environmentally friendly cooling water treatment in many countries (Leng et al., 2020, Mazumder Jafar, 2020, Liu et al., 2023). Among them, PESA was a new type of green water treatment agent with no phosphorus, no nitrogen, environmental protection and safety. It would not cause the problem of water environment eutrophication in long-term use (Liu et al., 2014, Leng et al., 2020, Yan et al., 2020, Shi et al 2012, Zhang et al., 2010).

* Corresponding author.
E-mail address: hualiyiwang@163.com (X. Liu).

https://doi.org/10.1016/j.arabjc.2024.106033
Received 22 July 2024; Accepted 20 October 2024
Available online 24 October 2024

PESA was originally developed as a scale inhibitor. It had strong inhibition ability to calcium ion, magnesium ion and iron ion, and was suitable for water treatment with high hardness and high alkalinity. In addition, PESA also had a certain effect on pipeline scaling, corrosion and other problems, and had biodegradability. Traditional corrosion inhibitors and scale inhibitors didn't have these advantages. However, PESA had some obvious defects, such as single functional group, which was limited in its application scope. Therefore, many researchers have carried out experimental studies on the modification of PESA to expand its application scope (Leng et al., 2020, Kadhim et al., 2021,Liu et al., 2020, Lai et al., 2020, Wei et al., 2022, Al-Itawi et al., 2019, Zhao et al., 2022, Zhang et al., 2021).

Gly contained hydroxyl and ester groups that chelate metal ions (such as calcium ions). This work aimed to introduce Gly into the molecular structure of PESA to obtain Gly-PESA. Because the existence of Gly can improve the corrosion and scale inhibition performance of PESA in a certain extent. The scale inhibition effects of Gly-PESA were studied by static experiments. The corrosion inhibition effect of Gly-PESA to Q235 carbon steel in cooling water was studied by static weight loss method. Nuclear magnetic hydrogen spectroscopy (^{1}H NMR), fourier transform Infrared spectroscopy (FTIR), thermogravimetric analysis (TGA), scanning electron microscopy (SEM), atomic force microscopy (AFM), X-ray photoelectron spectroscopy (XPS) and contact angle (CA) were used to characterize structures of Gly-PESA, the calcium scale or the surface of the steel test piece, which proved the scale inhibition and corrosion inhibition mechanism of Gly-PESA.

2. Experiment

2.1. Equipment and reagent

VERTEX7O Fourier Infrared Spectrometer (Bruker Technology Co., LTD., Germany) ; SIGMA300 Field Emission Scanning Electron Microscopy (Carl Zeiss AG, Germany) ; TGA-4000 Thermogravimetric Analyzer (PerkinElmer, USA) ; Zennium Pro Electrochemical Workstation (ZAHNER-elektrik GmbH & Co.KG, Germany) ; PulsarTM NMR Spectrometer (Shanghai Hao Lang Scientific Instrument Co., LTD., UK) ; JC2000 DM Contact Angle Measuring Instrument (Shanghai Zhongchen Digital Technology Equipment Co., LTD., China) ; AXIS SUPRA X-ray photoelectron Spectrometer (Shimadzu, Japan) and MFP-3D Origin Atomic Force Microscope (Oxford, UK).

Gly (Mass percentage 97 %) (Shanghai Yien Chemical Technology Co., LTD., China); Maleic anhydride, sodium hydroxide, anhydrous calcium chloride, anhydrous sodium sulfate, methanol, anhydrous ethanol, sodium bicarbonate, disodium EDTA (Tianjin Yongda Chemical Reagent Co., LTD. China), all of the above reagents were reagent grade and could be used without further purification; Corrosion pieces of Q235 carbon steel (Gaoyou Qinyou Instrument Chemical Co., LTD., area 20 cm^2, China).

2.2. Synthesis of PESA and Gly-PESA

The synthesis of PESA and Gly-PESA was carried out in reference (Leng et al., 2020. Wei et al., 2022. Zhang et al., 2021. Zhang et al., 2017.).

Epoxysuccinic acid (ESA) synthesis: First, 15 mL of distilled water was added to 9.8 g maleic anhydride, and 40 % NaOH solution was slowly added while stirring at 40 °C, and PH was controlled between 5–6. Secondly, added 0.6 g of sodium tungstate and sodium molybdate with a mass ratio of 1:1, droped 10 mL hydrogen peroxide at a slow rate, temperature rised to 65 °C, reaction for 2 h (the above is the cyclization reaction). Finally, the solution was adjusted to acid, then washed with methanol, extracted, filtered, obtained white solid (ESA) and dried for use at 40 °C.

PESA synthesis: Cyclization reaction solution was adjusted to about pH = 11, 0.4 g of initiator (calcium hydroxide) was added in four times, and the temperature was raised to 80 °C for 2 h. After the reaction, the solution was adjusted to acidity, washed with methanol for 5 times to obtain a viscous substance (PESA), and dried at 40 °C for use.

Gly-PESA synthesis: ESA and Gly were put into a three-mouth flask with a mass ratio of 1:0.33, and dissolved with distilled water, adjusting pH = 8. The initiator was added in four times (the amount was 8 % of the amount of reactant). After reaction lasted for 4 h at 80 °C, the solution was adjusted to neutral, and washed for 5 times with methanol. The obtaining viscous substance (Gly-PESA) was dried at 40 °C. The yield of Gly-PESA is about 60 %. The reaction process was shown in Fig. 1:

2.3. PESA and Gly-PESA structure analysis and sample characterization

The structures of Gly-PESA were analyzed by FTIR and ^{1}H NMR. The thermal stability of Gly-PESA was proved by TGA. SEM, XPS and FTIR were used to characterize $CaCO_3$ and $CaSO_4$. The surface morphology, film composition and wettability of the steel test pieces were analyzed by SEM, XPS, FTIR and CA.

2.4. Measurement of scale inhibition performance

The scale inhibition effects of PESA and Gly-PESA on $CaCO_3$ and $CaSO_4$ were compared and evaluated referring to the Chinese National standard (*GB/T16632-2019*) and literature (Liu et al., 2023). The scale inhibition performance test of $CaCO_3$ in the work: $\rho(Ca^{2+}) = 200$ mg/L and $\rho(HCO_3^-) = 400$ mg/L; The scale inhibition performance test of $CaSO_4$: $\rho(Ca^{2+}) = 2000$ mg/L, $\rho(SO_4^{2-}) = 4000$ mg/L.

2.5. Measurement of corrosion inhibition performance

The corrosion test water was tap water [Tangshan,Heiei]: pH=7.8, total hardness was 190 mg/L, conductivity was 624 μs/cm, and the concentrations of Ca^{2+}, Mg^{2+}, Cl^- and SO_4^{2-} were 54.8 mg/L, 27.3 mg/L, 33 mg/L and 60 mg/L respectively. The prepared steel test pieces were immersed in a beaker containing 500 mL simulated cooling water and different doses of Gly-PESA at 30 °C. After soaking for 24 h, removed the steel test pieces, washed (first with 5 % HCl and 3 mg/L hexamethylenetetramine, followed by deionized water), dried, and weighed. Refer to test method of literature (Liu et al., 2023), the corrosion rate(X) and the corrosion inhibition efficiency (η) were calculated. The formulas were (1) and (2).

$$X = \frac{W}{S \times T} \tag{1}$$

$$\eta(\%) = \frac{X_0 - X}{X_0} \times 100 \tag{2}$$

where, X ($g/cm^2 \cdot h$), W- lost weight (g),S-area (cm^2), T-time (h), X, X_0 – corrosion rate with or without PESA-Lcy-Sea.

3. Results and discussion

3.1. Structural characterization of Gly-PESA

The FTIR, ^{1}H NMR and TGA of Gly-PESA were showed in Fig. 2. In the infrared spectrum of PESA in Fig. 2(a), 3477 cm^{-1}/3381 cm^{-1} and 1627 cm^{-1}/1398 cm^{-1} were O−H and C═O stretching vibration absorption peaks in –COOH, respectively. 1315 cm^{-1} was C−H deformation vibration, and 1066 cm^{-1} was C−O−C stretching vibration absorption peak. In the infrared spectrum of Gly-PESA, the hydroxyl peak becomed wider at 3435 cm^{-1}, the absorption peak of $-CH_2-$ was increased at 2932 cm^{-1}, and the peak of C═O at 1627 cm^{-1} and the peak of C−H at 1315 cm^{-1} became larger. Therefore, FTIR analysis shows that Gly-PESA was successfully obtained.

In ^{1}H NMR of Gly-PESA in Fig. 2(b), besides containing the characteristic peaks in PESA, hydrogen peaks in methylene (−CH_2−) and

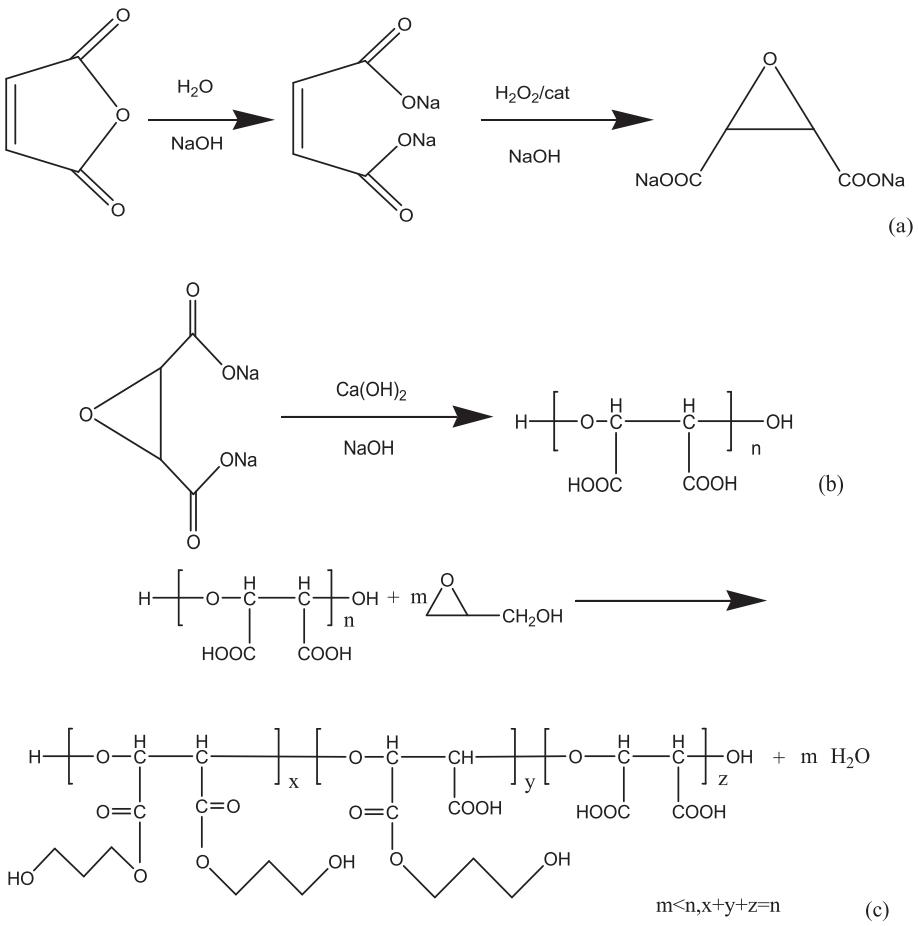

Fig. 1. Synthesis of ESA(a), PESA(b) and Gly-PESA(c).

hydroxyl ($-CH_2OH$) in Gly were also found at the chemical shift $\delta = 3.5$ ppm and $\delta = 1.5$ ppm, respectively, which proved the successful synthesis of Gly-PESA.

Fig. 2(c) was the TGA diagram of Gly-PESA and PESA. It could be seen from the TGA curve in Fig. 2(c) that the stability of Gly-PESA and PESA is basically the same. According to the TGA figure of Gly-PESA, the weight loss was smooth at 30 °C–250 °C, which may be caused by the volatilizing of water or other volatile substances, and the weight loss rate was about 10 %–12 %.The weight loss rate was about 28 % at 250 °C–300 °C, which may be due to the fracture of the branch chain of Gly-PESA. Subsequently, the weight loss was gentle between 300 °C and 500 °C, and further gentler between 500 °C and 700 °C, which may be due to the further increase of temperature leading to the break of the main chain of a few Gly-PESA molecules. At 700 °C-800 °C, weight loss was rapid, probably because the temperature was too high to cause many Gly-PESA molecules to decompose faster (Liu et al., 2023). In summary, Gly-PESA had excellent thermal stability in the range of 0 °C-250 °C, and could meet the needs of industrial production.

3.2. Gly-PESA scale inhibition performance analysis

3.2.1. Influence of the dosage of Gly-PESA on the scale inhibition performance to $CaCO_3$ and $CaSO_4$

By changing the dosage of Gly-PESA, the scale inhibition effect to $CaCO_3$ was shown in Fig. 3(a). When the dosage of Gly-PESA was 2 mg/L, the scale inhibition efficiency was 45.7 %. Moreover, with the increase of the dosage of Gly-PESA (2 mg/L–12 mg/L), the scale inhibition efficiency was continuously improved, and the scale inhibition performance of Gly-PESA was obviously better than that of PESA. When the dosage of Gly-PESA was 8 mg/L and 10 mg/L, respectively, the scale inhibition efficiency reached 90.3 % and 98.0 %, respectively. In contrast, the scale inhibition efficiency of Gly-PESA was increased by 10.8 % and 7.7 % over that of PESA, respectively. This was due to the existence of polar groups in Gly-PESA, which enhanced its electrostatic attraction and chelation with calcium ions in water, thus forming a stable calcium ion complex in water, reducing the formation of sediments, and further improving the scale inhibition efficiency (Yan et al., 2020; Zhang et al., 2021; Wang et al., 2017).

By changing the dosage of Gly-PESA, the scale inhibition efficiency to $CaSO_4$ was shown in Fig. 3(b). It can be seen from Fig. 3(b) that the scale inhibition efficiency of Gly-PESA increased with increasing dosage. When the dosage of Gly-PESA was 10 mg/L, the scale inhibition efficiency of Gly-PESA was 92.6 %, and the scale inhibition efficiency of Gly-PESA was 13.8 % higher than that of PESA. When the dosage exceeded 10 mg/L, the scale inhibition efficiency of Gly-PESA increased little. In conclusion, the inhibition effect of Gly-PESA to $CaSO_4$ was better than that of PESA.

3.2.2. Effect of temperature on the scale inhibition of Gly-PESA to $CaCO_3$ and $CaSO_4$

The test temperature would affect the formation rate and solubility of $CaCO_3$ and $CaSO_4$ in the system. Therefore, in this work, the concentration of PESA and Gly-PESA was 10 mg/L respectively to study the influence of temperature on the scale inhibition ability of Gly-PESA, and the test results were shown in Fig. 4. Fig. 4 showed that the scale inhibition ability of PESA and Gly-PESA on $CaCO_3$ [Fig. 4(a)] and $CaSO_4$ [Fig. 4(b)] both decreased with the increase of test temperature, but the decrease of Gly-PESA was very small. Moreover, the scale inhibition efficiency of Gly-PESA was always greater than that of PESA for both $CaCO_3$ and $CaSO_4$. This may be because PESA and Gly-PESA adsorb

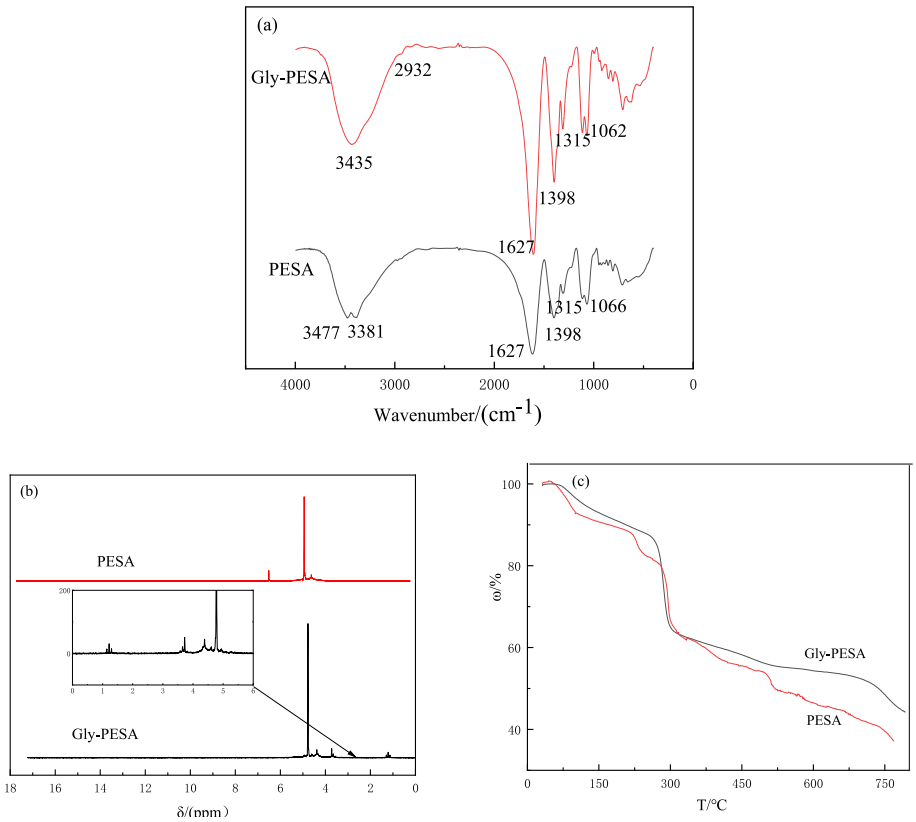

Fig. 2. The FTIR(a),^{1}H NMR(b) and TGA(c) of PESA and Gly-PESA.

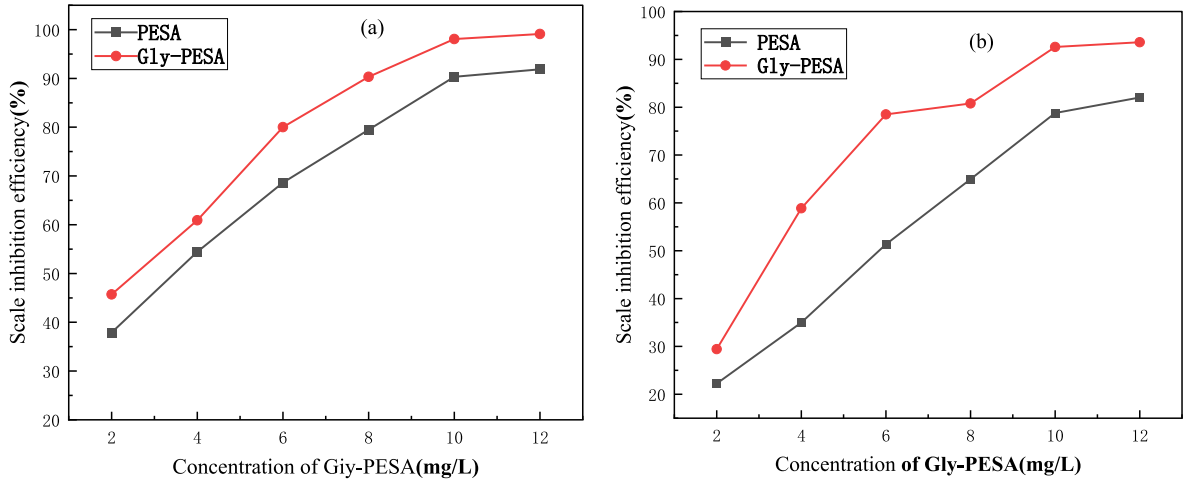

Fig. 3. Scale inhibition performance of with different dosage of PESA and Gly-PESA to $CaCO_3$(a) and $CaSO_4$(b).

small crystals of calcium scale to release heat, so the increase of system temperature would affect the adsorption amount of PESA and Gly-PESA on small crystals (Liu et al., 2018). In addition, with the increase of system temperature, the velocity of the ion in the system also accelerated, making it easier for forming scale crystals. However, when the temperature was 80 °C, the scale inhibition efficiency of Gly-PESA on $CaCO_3$ and $CaSO_4$ could reach 88.3 % and 85.7 %, respectively. This indicated that Gly-PESA could maintain a good scale inhibition effect at high system temperature.

3.2.3. *Effect of Ca^{2+} concentration on the resistance of Gly-PESA to $CaCO_3$ and $CaSO_4$*

With the extension of the use of industrial circulating cooling water, the Ca^{2+} concentration in water will increase. Based on national standard (GB/T16632-2019) in China and the literature (Htet and Zeng, 2022; Zhang et al., 2017; Liu et al., 2023), the concentration range of Ca^{2+} was selected 200 mg/L-600 mg/L(for $CaCO_3$) and 2000 mg/L-6000 mg/L(for $CaSO_4$) in this work. Therefore, this work studied the effects of Gly-PESA (10 mg/L) on the scale inhibition properties to $CaCO_3$ and $CaSO_4$ at different Ca^{2+} concentrations, as shown in Fig. 5. As couuld be seen from the curve in Fig. 5, with the increase of Ca^{2+} concentration, the scale inhibition efficiency of Gly-PESA on $CaCO_3$

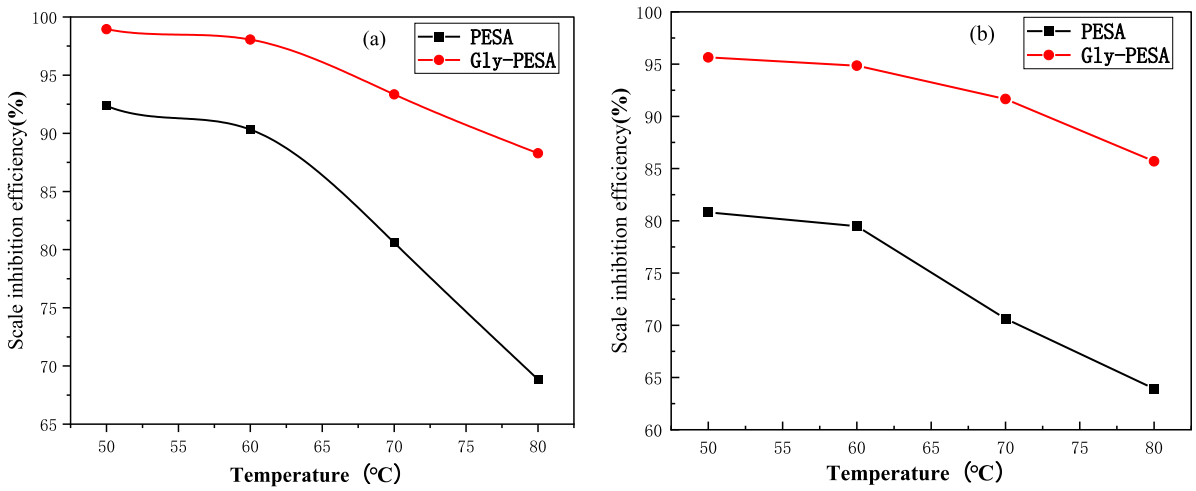

Fig. 4. Effects of PESA(Dosage of 10 mg/L) and Gly-PESA(Dosage of 10 mg/L) on the scale inhibition properties of (a) $CaCO_3$ and (b) $CaSO_4$ at different temperatures.

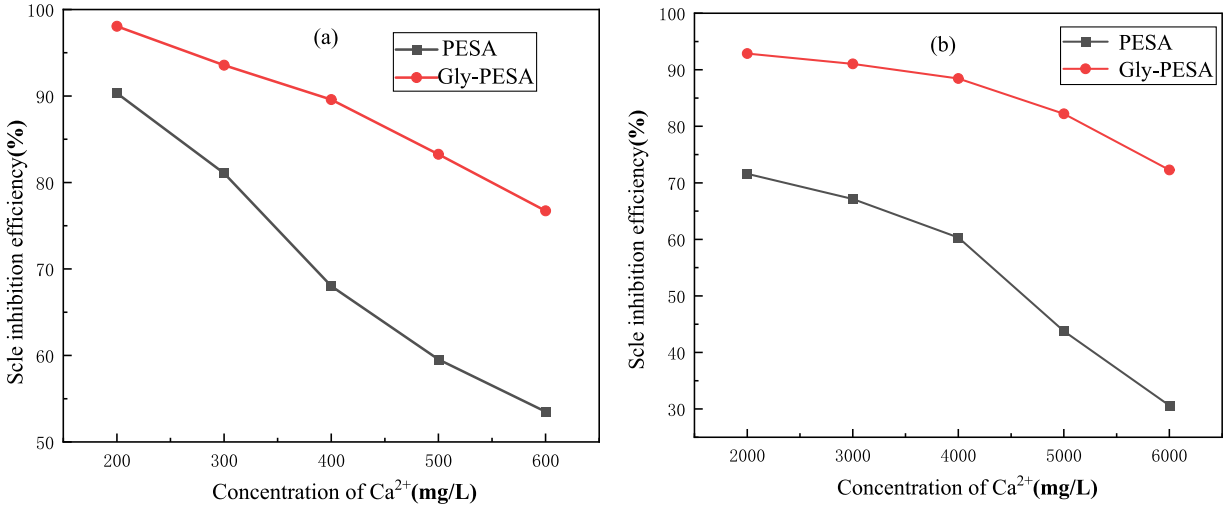

Fig. 5. Effects of PESA(Dosage of 10 mg/L) and Gly-PESA(Dosage of 10 mg/L) on the scale inhibition properties of (a) $CaCO_3$ and (b) $CaSO_4$ at different Ca^{2+} concentrations.

[Fig. 5(a)] and $CaSO_4$ [Fig. 5(b)] gradually decreased, but the scale inhibition capacity of Gly-PESA was always stronger than that of PESA. According to the data of $CaCO_3$ in Fig. 5(a), when the Ca^{2+} concentration reached 500 mg/L, the scale inhibition efficiency of Gly-PESA could still reach 83.2 %, while the PESA could only reach 59.6 %. According to the data of $CaSO_4$ in Fig. 5(b), when the Ca^{2+} concentration reached 5000 mg/L, the scale inhibition efficiency of Gly-PESA could still reach 82.2 %, while the PESA could only reach 43.8 %. Therefore, it could be concluded that the scale inhibition capacity of PESA and Gly-PESA on $CaCO_3$ and $CaSO_4$ were closely related to the concentration of Ca^{2+} in the system, but the tolerance of Gly-PESA to calcium ions was always better than that of PESA.

3.3. Structural characterization of calcium scale

In order to further demonstrate the scale inhibition performance of Gly-PESA, SEM, FTIR and XPS were used to characterize the changes of crystal structure of $CaCO_3$ and $CaSO_4$.

3.3.1. SEM characterization of $CaCO_3$ and $CaSO_4$

$CaCO_3$ crystals were prepared in blank system, systems with PESA and Gly-PESA, respectively. The SEM of $CaCO_3$ crystals was shown in Fig. 6. As can be seen from Fig. 6(a) and Fig. 6(b), $CaCO_3$ in the blank group was mainly composed of hexahedral calcite, with a smooth surface and hard texture. Although the crystal pattern of calcium scale added with PESA and Gly-PESA both changed greatly, the crystal distortion of calcium scale with Gly-PESA was more obvious, the crystal growth rule was destroyed, the particles became fine, and showed a good dispersion state, which indicated that Gly-PESA had a stronger interference on the formation of $CaCO_3$ (Liu et al., 2023).

The SEM of $CaSO_4$ in the blank system and the scale inhibition system with PESA and Gly-PESA was shown in Fig. 7. As shown in Fig. 7(a) and Fig. 7(b), the crystals in the blank group were regular columnar structures with smooth surfaces. When PESA was added, the crystals in Fig. 7(c) and Fig. 7(d) became small, irregular shapes. When Gly-PESA was added, the crystal in Fig. 7(e) and Fig. 7(f) had no fixed shape, and the crystal structure was more loose. More specifically, $CaSO_4$ crystals were completely broken into a small and unstable powder state.

After the addition of scale inhibitor, SEM shows that the crystal structure of $CaCO_3$ and $CaSO_4$ changes. Probably mainly because (i) the complex of scale inhibitor molecules and Ca^{2+} ions in water formed a stable water-soluble chelate, thereby reducing the concentration of free

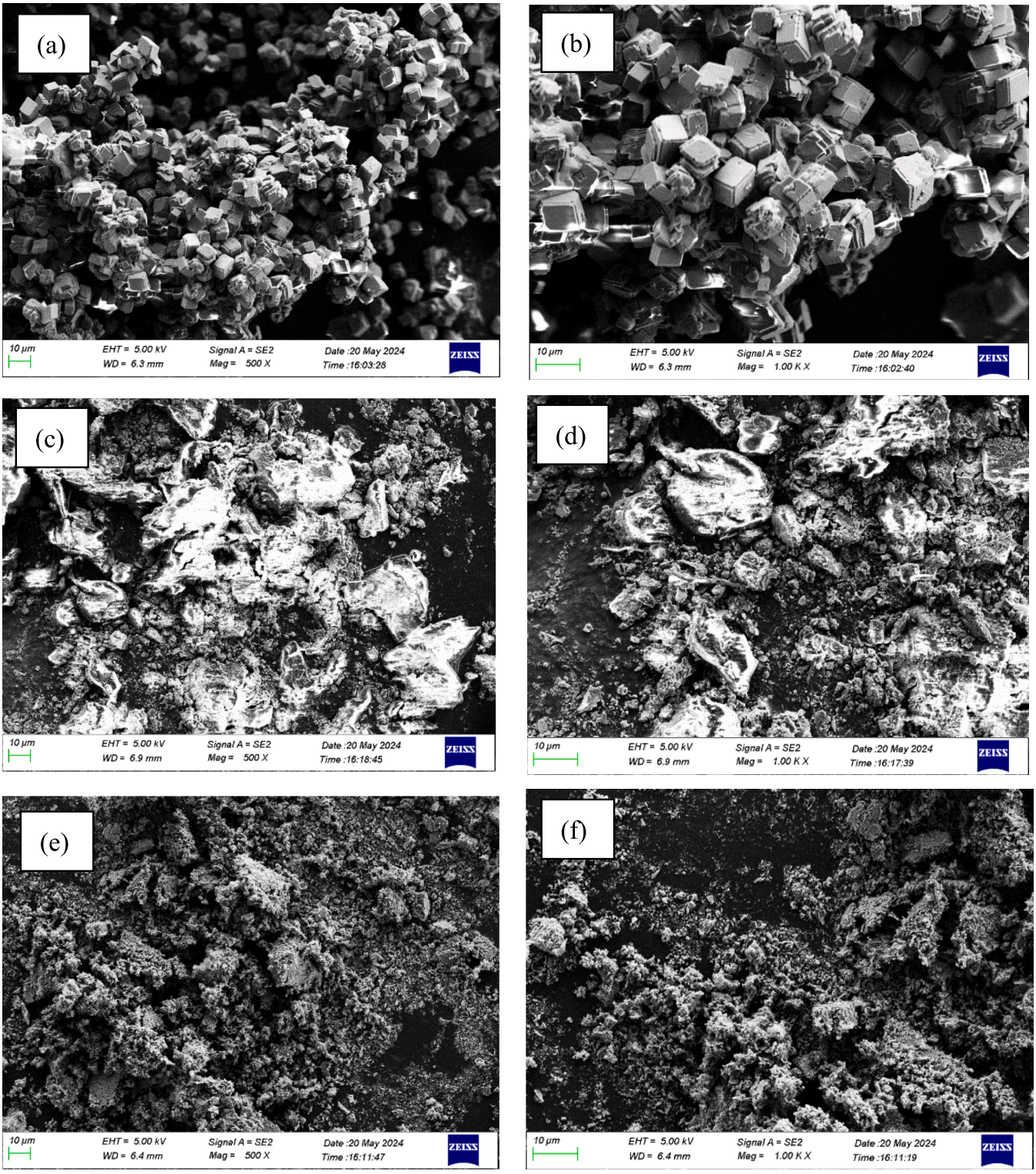

Fig. 6. SEM of $CaCO_3$ crystals. [Blank system: (a)/(b); System with PESA(10 mg/L): (c)/(d); System with Gly-PESA(10 mg/L): (e)/(f)].

calcium ions in water. (ii) the scale inhibitor molecules were adsorbed on the active growth point of microcrystals, which led to distortion of calcium scale crystals and increased of internal stress, preventing crystal aggregation and deposition (Liu et al., 2023; Htet T. T. et al., 2022).

3.3.2. *FTIR result of $CaCO_3$ and $CaSO_4$*

FTIR analysis was performed in this work in order to further confirm the crystal structures of $CaCO_3$ and $CaSO_4$.

The crystal types of $CaCO_3$ were different when different scale inhibitors are added to the scale inhibition system. The FTIR spectrum of $CaCO_3$ crystals were shown in Fig. 8(a), where the adsorption peaks at 711 cm^{-1} and 873 cm^{-1} represented the stable calcite and unstable aragonite crystal states of $CaCO_3$, respectively (Meng et al., 2007, Naka, 2003). It was obvious from Fig. 8(a) that $CaCO_3$ in the blank group was mainly calcite (only a small amount of aragonite), while the $CaCO_3$ added with PESA and Gly-PESA was mainly aragonite (only a small

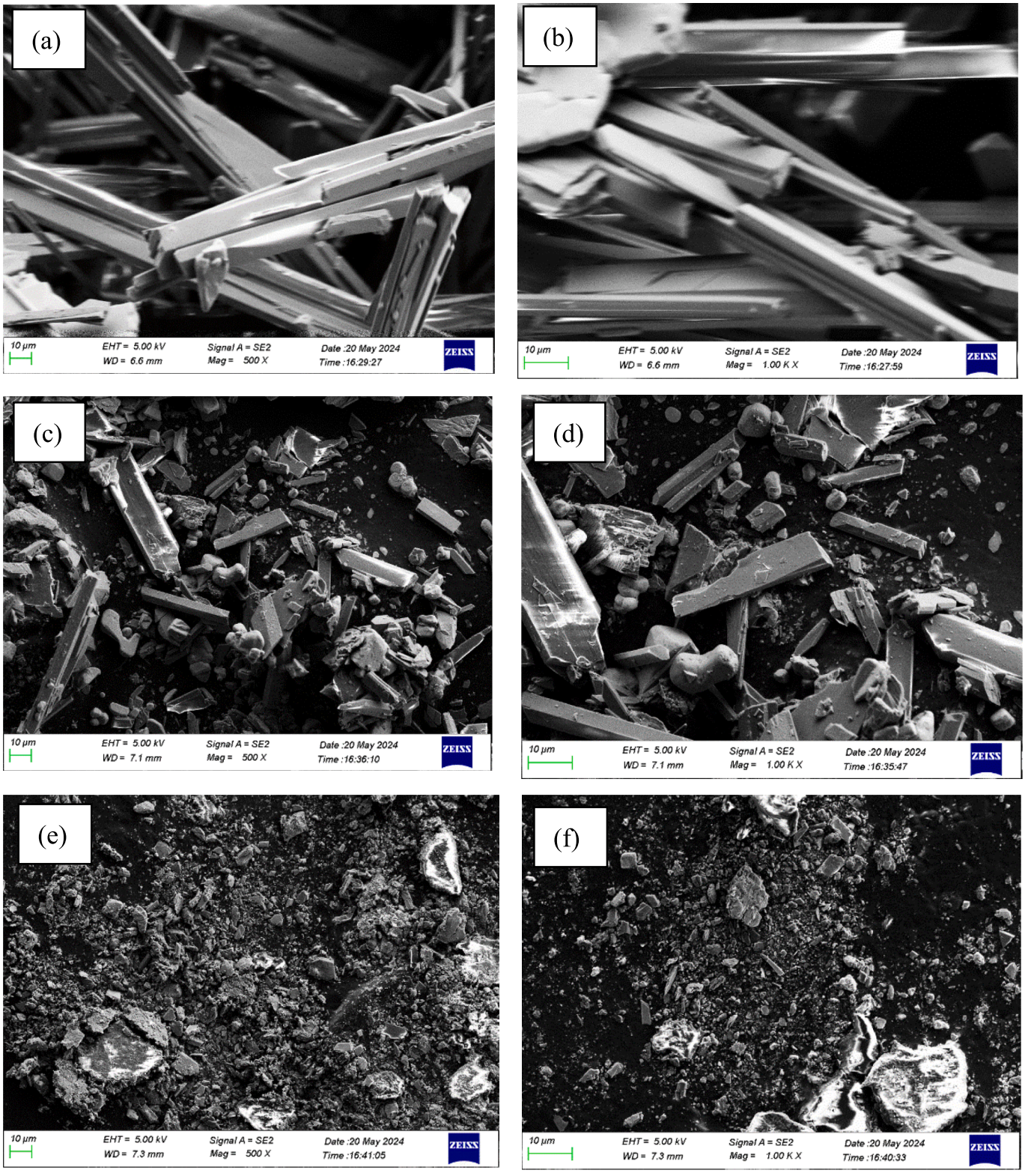

Fig. 7. SEM of $CaSO_4$ crystals. [Blank system: (a)/(b); System with PESA(10 mg/L): (c)/(d); System with Gly-PESA(10 mg/L):(e)/(f)].

amount of calcite). This was because the scale inhibitor molecules interfered with the process which aragonite formed calcite (Meng et al., 2007). In addition, it could be further seen from Fig. 8(a) that the peak of aragonite with Gly-PESA was significantly larger than that of adding PESA, indicating that Gly-PESA had a better scale inhibition effect. This phenomenon could be explained that the adsorption capacity of Gly-PESA on the surface of $CaCO_3$ was obviously stronger than that of PESA, which showed strong lattice distortion. Fig. 8(b) showed that the peaks of $CaSO_4$ scale obtained in different systems were consistent, indicating that the crystal type of $CaSO_4$ did not change, but the strength of the peaks changed, and the peaks with Gly-PESA were smaller than those with PESA, indicating that the crystallinity of $CaSO_4$ in the system with Gly-PESA was worse. This showed that Gly-PESA had better scale inhibition effect on $CaSO_4$ (Zhang et al., 2017, Nan et al., 2022).

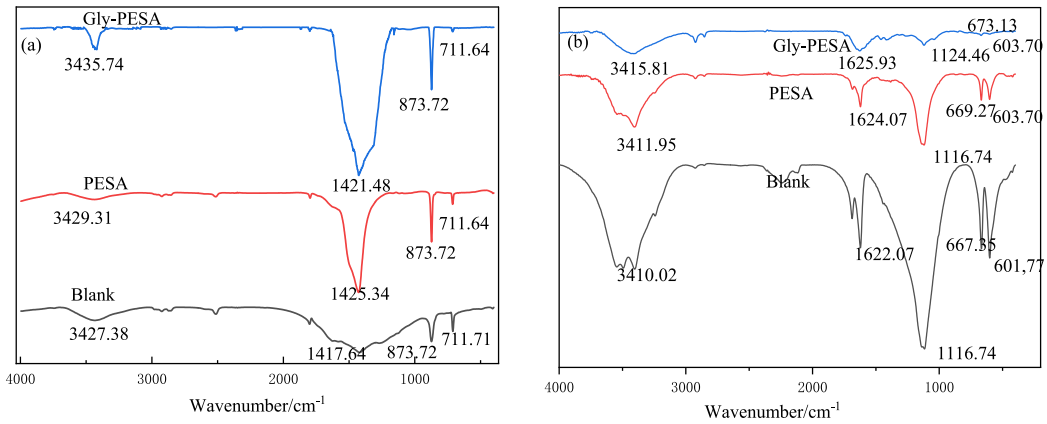

Fig. 8. FTIR of $CaCO_3$ (a) and $CaSO_4$ (b) in different systems without or with PESA(10 mg/L) or Gly-PESA(10 mg/L).

3.3.3. *XPS characterization of $CaCO_3$ and $CaSO_4$ scale*

In order to further explore the adsorption properties of Gly-PESA, we performed XPS analysis of O1*s* and Ca2*p* of $CaCO_3$ and $CaSO_4$ formed in different systems.

Fig. 9 showed the O1*s* XPS spectra of $CaCO_3$ and $CaSO_4$. In addition to the main O peaks of $CaCO_3$ and $CaSO_4$ at 529 eV (Fig. 9(a), (d)) in blank system, peaks of C−O(527 eV) and C═O(529.91 eV, 530.56 eV) appeared in Fig. 9(b)/(c)/(e)/(f) after the addition of PESA and Gly-PESA. This again proved that PESA and Gly-PESA adsorbed active sites on the surface of $CaCO_3$ and $CaSO_4$ and interfered with their growth (Zhang et al., 2021). Fig. 10 showed the Ca2*p* XPS spectra of $CaCO_3$ and $CaSO_4$ scale. In the blank system, the Ca2*p* spectra of $CaCO_3$ had significant characteristic peaks at 344.38 eV and 347.99 eV respectively. In the system with PESA, the peak displacement of *Ca2p* spectra was 343.82 eV and 347.47 eV, which might be the change of Ca^{2+} chemical environment causing the variation of scale crystal pattern. In the system with Gly-PESA, the peak displacement of Ca2*p* spectra was 345.18 eV and 348.72 eV, which further proved that Gly-PESA changed the crystal structure of $CaCO_3$ (Zhang et al., 2023). The addition of PESA caused the Ca2*p* peak of $CaSO_4$ to move by 0.18 eV relative to the blank Ca2*p* peak, while the addition of Gly-PESA caused the Ca2*p* peak to move by 0.20 eV and 0.17 eV relative to the blank Ca2*p* peak, respectively, as shown in Fig. 10(e) and Fig. 10(f). These results showed that the addition of Gly-PESA could cause changes of the chemical environment around Ca^{2+}, and the effective groups of Gly-PESA could chelate with Ca^{2+}, increase the electron density around Ca^{2+}, and make the calcium peak migrate (Zhang et al., 2023). The above SEM, FTIR and XPS data results showed that Gly-PESA could be adsorbed on the surface of $CaCO_3$ and $CaSO_4$, affecting the surface morphology and transformation path of crystals, thus effectively inhibiting their formation and deposition in solution.

3.4. *Study on corrosion inhibition performance of Gly-PESA*

In this section, weight-loss method, SEM, FTIR, CA and XPS were used to evaluate the corrosion inhibition performance of Gly-PESA.

3.4.1. *Weight-loss method*

In this section, the corrosion inhibition efficiency of Gly-PESA and PESA with different dosage was measured by weight loss method. The experimental results were shown in Table 1. It can be seen that with the increase of the dosage of Gly-PESA and PESA, the corrosion rate decreased and the corrosion inhibition efficiency increased. When the concentration of Gly-PESA and PESA was 400 mg/L, η_{max} reached 78.17 % and 67.05 %, respectively. This was because the steel surface area covered by Gly-PESA with branched chains was larger, and the chemisorbed effect was stronger.

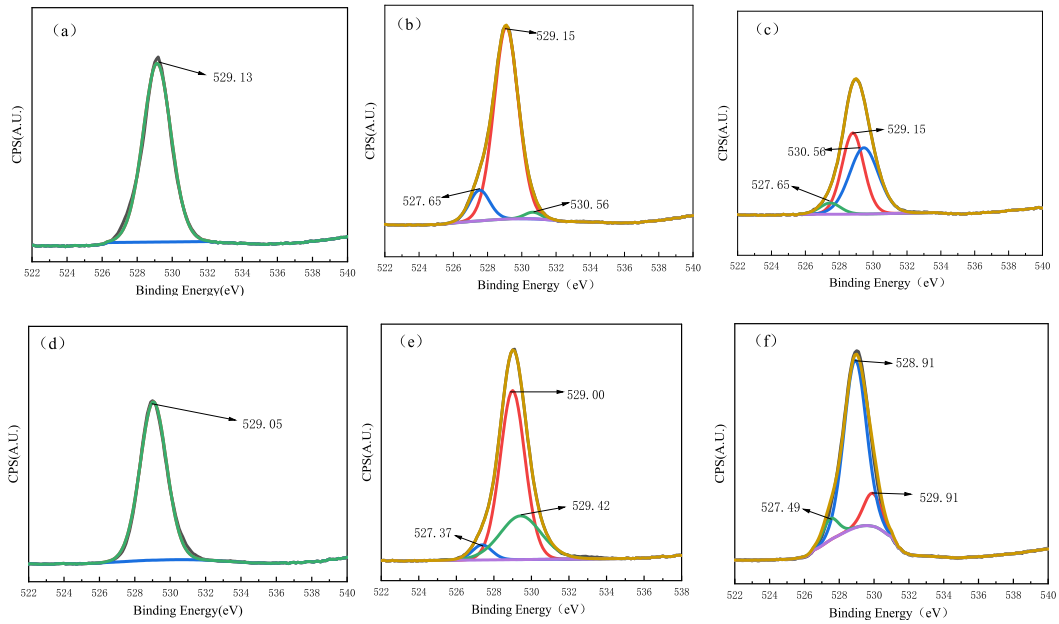

Fig. 9. O1*s* XPS of $CaCO_3$ (a-c)and $CaSO_4$(d-f). [(a)/(d) Blank system, (b)/(e) System with PESA(10 mg/L), (c)/(f) System with Gly-PESA(10 mg/L)].

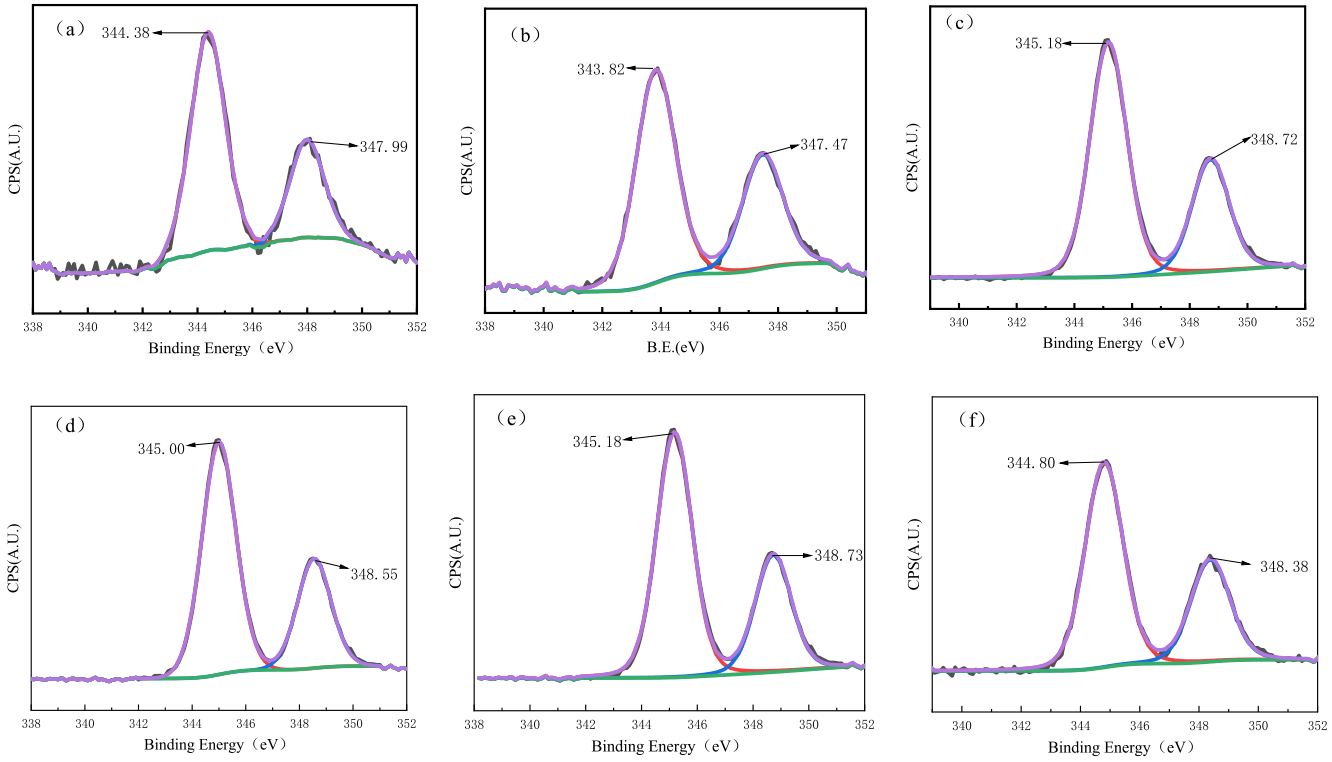

Fig. 10. Ca2*p* XPS of $CaCO_3$(a-d) and $CaSO_4$(d-f). [(a)/(d) Blank system, (b)/(e) System with PESA(10 mg/L), (c)/(f) System with Gly-PESA(10 mg/L)].

Table 1
Corrosion inhibition performance of Gly-PESA and PESA.

Gly-PESA			PESA	
C_{Inhi}	X (g/cm^2.h)	η (%)	X (g/cm^2.h)	η (%)
0	2.96×10^{-5}	/	2.96×10^{-5}	/
50	1.74×10^{-5}	41.31	1.88×10^{-5}	36.56
100	1.39×10^{-5}	53.03	1.54×10^{-5}	48.01
200	1.06×10^{-5}	64.18	1.33×10^{-5}	55.12
300	8.40×10^{-6}	71.63	1.15×10^{-5}	61.14
400	6.46×10^{-6}	78.17	9.75×10^{-6}	67.05

Firstly, from the point of view of scale and corrosion inhibition: the scale inhibition performance of Gly-PESA synthesized in this work was better than that of arginine-modified PESA[Arg-PESA] in the literature (Zhang et al., 2021), especially in terms of being affected by different temperature and calcium ion concentration. Second, the corrosion inhibition efficiency of Gly-PESA for Q235 steel could reach 78.17 %. the corrosion inhibition performance of Gly-PESA was basically equivalent to that of Arg-PESA (Zhang et al., 2021). The corrosion inhibition efficiency also reached a medium level.Therefore, the Gly-PESA synthesized in this work had the dual function of scale inhibition and corrosion inhibition. In the following research work, in order to further enhance the corrosion inhibition performance of GLY-PESA, this research group will further carry out the compounding work of GLY-PESA.

3.4.2. Surface analysis of the steel test pieces

The surface analysis technique was used to describe the surface state of Q235 steel and to prove the adsorption performance of Gly-PESA. The surface analysis methods we used were SEM, FTIR, AFM, XPS and CA.

1) SEM and FTIR

Fig. 11(a–c) showed the SEM images of the surface of the steel test pieces before corrosion, in the blank system and in the Gly-PESA system added 400 mg/L. The surface of the steel test piece (before corrosion) had obvious grinding marks and was smooth; The surface of the steel test piece (soaked in the blank solution) was covered with corrosion products. After the addition of Gly-PESA, the damage of the test piece was significantly reduced, the surface became smooth, and the corrosion products were less, which could be inferred that Gly-PESA played a protective role on the surface of the test piece.

The FTIR spectra of Gly-PESA and the surface of the test piece (soaked in Gly-PESA solution) were shown in Fig. 11(d). As shown in Fig. 11(d), there were O–H stretching vibration absorption peaks in carboxyl group (3435 cm^{-1}), $-CH_2-$ functional group absorption peaks (2932 cm^{-1}, 2859 cm^{-1}), C═O stretching and deformation vibration absorption peaks in carboxyl group (1627 cm^{-1}, 1388 cm^{-1}) and C−O−C tensile vibration absorption peak (1051 cm^{-1}) in the FTIR spectrum of the surface of the test piece. Compared with the FTIR diagram of Gly-PESA, it could be inferred that the functional groups of Gly-PESA acted on the metal surface to prevent corrosion reactions due to its adsorption.

2) AFM

AFM was used to study the surface morphology of the test pieces before corrosion, in blank solution and in solution with Gly-PESA, as shown in Fig. 12. It could be clearly seen from Fig. 12 that the steel surface (before corrosion) was the smoothest, and its average surface roughness was 1.88 nm, as shown in Fig. 12(a, b). In the blank system, the height of the steel surface fluctuated greatly, forming the shape of mountains and hills, whose average surface roughness was 12.79 nm, as shown in Fig. 12(c, d). The surface height fluctuation of the steel protected by Gly-PESA was gentler than that of the blank system, and the damage degree was lower, and the average surface roughness was 5.11 nm, as shown in Fig. 12(e, f). In Fig. 12(g), the fluctuation amplitude of the corresponding height profile of the steel surface: steel sheet before corrosion < steel surface in the system with Gly-PESA<steel surface in blank system. The height fluctuation amplitude of the steel surface in the system with Gly-PESA was significantly lower than that of the blank

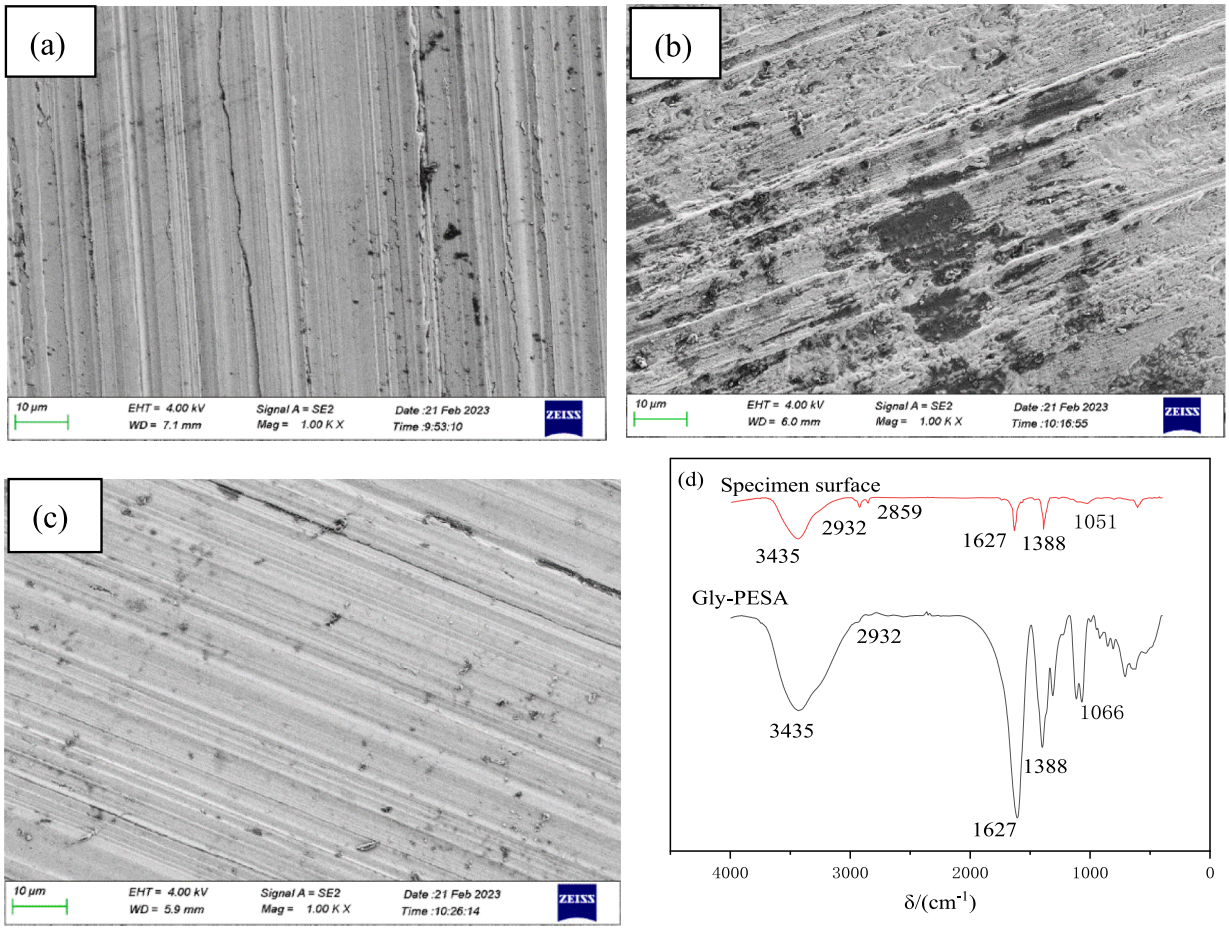

Fig. 11. SEM (a-c) and FTIR (d) on Q235 steel surface [(a) before corrosion; (b) blank system (c) System with Gly-PESA(400 mg/L); (d) System with Gly-PESA(400 mg/L)].

system, indicating that the corrosion rate of the steel was significantly reduced. In summary, the micromorphology of AFM confirmed the results of gravimetric analysis (Gly-PESA has good corrosion inhibition performance), and it could be inferred that Gly-PESA formed a protective film on the steel surface, which had low permeability to corrosive ions and had a good protection ability against steel corrosion.

3) CA

CA is an angle formed when the liquid was droped onto a metal surface and can be used to characterize the wettability of a metal surface. In this work, the wettability of metal surface before and after corrosion was expressed by measurement of CA, which the corrosion inhibition performance of Gly-PESA was verified. For the test pieces, the values of CA were 118°(before corrosion), 55.5°(blank) and 92.0°(with Gly-PESA) respectively, as shown in Fig. 13. From the value of CA, it could be concluded that the hydrophobicity of the metal surface in the presence of Gly-PESA was somewhat weakened compared with the metal surface (before corrosion), but it was much enhanced compared with the metal surface (in the blank solution). This was due to the fact that the Gly-PESA molecules adsorbed and formed a protective layer on the steel surface. Therefore, the presence of Gly-PESA slowed down the corrosion of steel and improved the corrosion inhibition efficiency.

4) XPS

XPS was a powerful technique for detecting the bonding information of corrosion inhibitors on metal surfaces. Therefore, XPS measurements were performed on the steel test piece immersed in solution with Gly-PESA. Fig. 14 showed the XPS scanning full spectrum and high resolution spectrum of the steel surface. As shown in Fig. 14a, Fe, C and O elements existed on the surface of the steel test piece. In Fig. 14b, the *Fe2p*$_{3/2}$ spectrum had three main peaks. The peak at 705.21 eV was attributed to metallic iron (Qiang et al., 2021). The peak value of 708.91 eV was related to $FeCl_2$ and FeOOH (Qiang et al., 2021). In addition, the peak of 724.22 eV was attributed to Fe_2O_3 and $FeCl_3$ (Wan et al., 2022). The spectrum of *C1s* (Fig. 14c) had three peaks. 284.70 eV was C−C or C−H, 285.80 eV was C−O or C−O−C, and 288.30 eV was C═O (Wan et al., 2022, Aah et al., 2020). The *O1s* spectrum (Fig. 14d) was decomposed into three peaks. The peak at 526.50 eV corresponded to the oxide of iron, the peak at 528.80 eV corresponded to C−O−C, forming a hydrated iron oxide (i.e. FeOOH), and the peak at 530.5 eV was C−OH, the corresponding compound was a complex of water and iron salts (Qiang et al., 2021, Aah et al., 2020, Gu et al., 2023). XPS further demonstrated that Gly-PESA formed a protective film on the steel surface and prevented the steel from being corroded.

3.5. Analysis of corrosion inhibition mechanism

In order to investigate the inhibition mechanism of Gly-PESA, adsorption isothermal equation was used for further analysis. In addition, the whole corrosion inhibition process was explained in detail.

3.5.1. Adsorption isotherm

The corrosion inhibition performance of the organic corrosion inhibitor mainly depended on its adsorption effect on the metal surface. Therefore, in order to explain the corrosion inhibition mechanism, the uses of adsorption isotherms such as Langmuir, Floy-Huggin, Bockris-

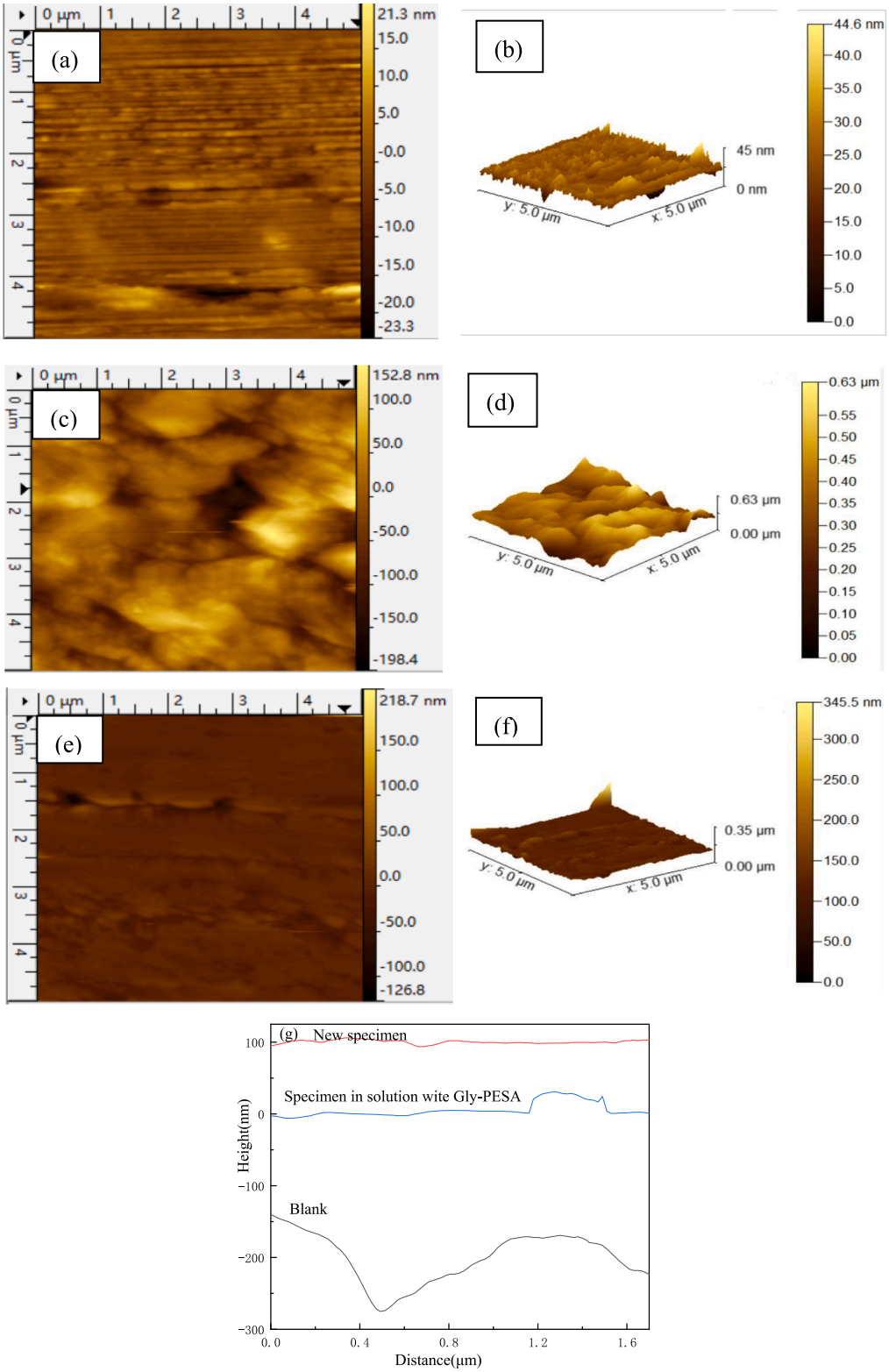

Fig. 12. AFM of Q235 steel surface [(a/b) before corrosion; (c/d) blank system; (e/f) System with Gly-PESA(400 mg/L); (g) corresponding height distribution on Q235 steel surface of new sppecimen and without or with Gly-PESA(400 mg/L)].

Swinkels, Frumkin and Temkin isotherms were an effective method (Liu et al., 2023). More specifically, we chose the Langmuir formula for the experiment because it had the best degree of fitting. Therefore, other isotherms weren't considered.

$$\frac{C_{inh}}{\theta} = \frac{1}{K_{ads}} + C_{inh} \tag{3}$$

where, C_{inh} was the concentration of Gly-PESA (g/L), K_{ads} was the equilibrium constant of the adsorption process (L/g), θ was the surface

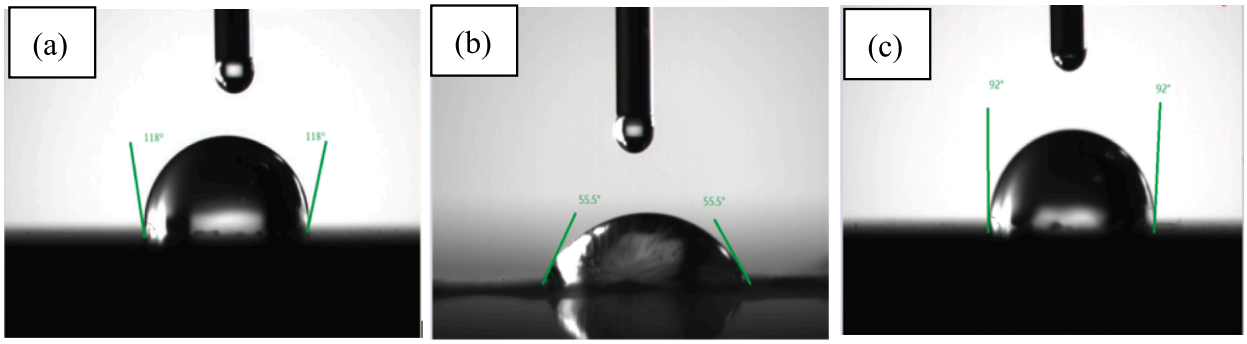

Fig. 13. CA of Q235 steel surface [(a) before corrosion; (b) blank system; (c) System with Gly-PESA(400 mg/L)].

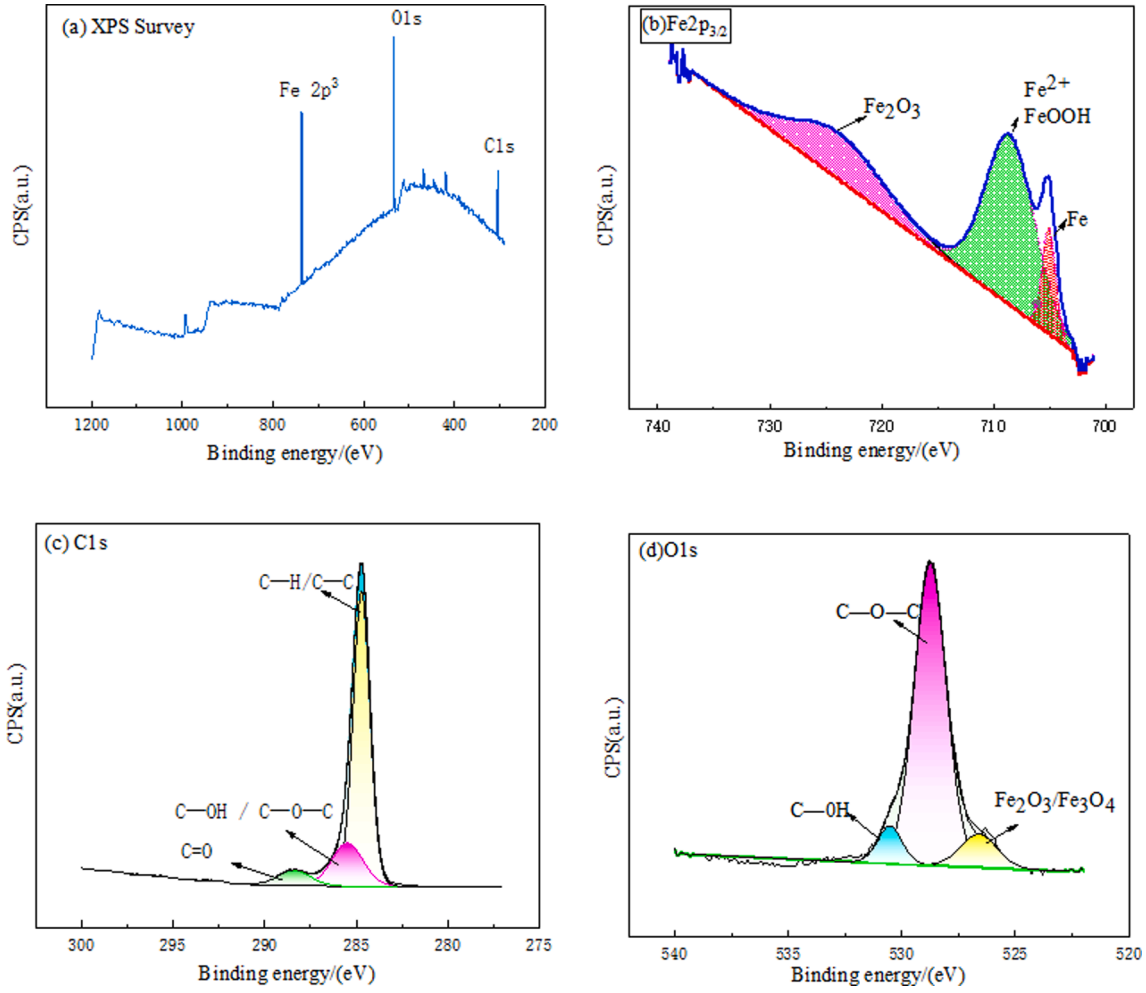

Fig. 14. XPS diagram of Q235 steel after soaking in solution with Gly-PESA(400 mg/L) [(a) XPS survey; (b)Fe2$p_{3/2}$; (c)C1*s*; (d)O1*s*].

coverage of Gly-PESA molecules on the steel surface, which was equal to the value of corrosion inhibition efficiency obtained by the weight loss method.

According to equation (3), Fig. 15 depicted the relationship between C_{inh}/θ and C_{inh}, and the discrete points were fitted into a straight line, with the correlation coefficient $R^2 = 0.99417$. This indicated that the adsorption behavior of Gly-PESA molecules conformed to Langmuir formula, indicating that the interaction between molecules can be ignored. The following further used K_{ads} to calculate the adsorption free energy ΔG^0_{ads}:

$$\Delta G^0_{ads} = -RT\ln(1 \times 10^3 K_{ads}) \quad (4)$$

where R=8.314 J/ (mol·K), T=303 K, and C_{H2O}=1 × 10^3 g/L. The calculated results of K_{ads} and ΔG^0_{ads} were 13.2398 L/g and − 23.9091 kJ/mol, respectively.

$|\Delta G^0_{ads}| \leq 20$ kJ /mol and $|\Delta G^0_{ads}| \geq 40$ kJ/mol were the physical adsorption and chemical adsorption of corrosion inhibitor molecules on metal surface, respectively (Liu et al., 2023; Belkheiri et al., 2024). Based on the above data, it could be concluded that the adsorption behavior of Gly-PESA on the steel surface includes physical adsorption and chemical adsorption. More specifically, in terms of physical adsorption, there was electrostatic attraction when the Gly-PESA molecule was close to the steel surface. In terms of chemisorption, the

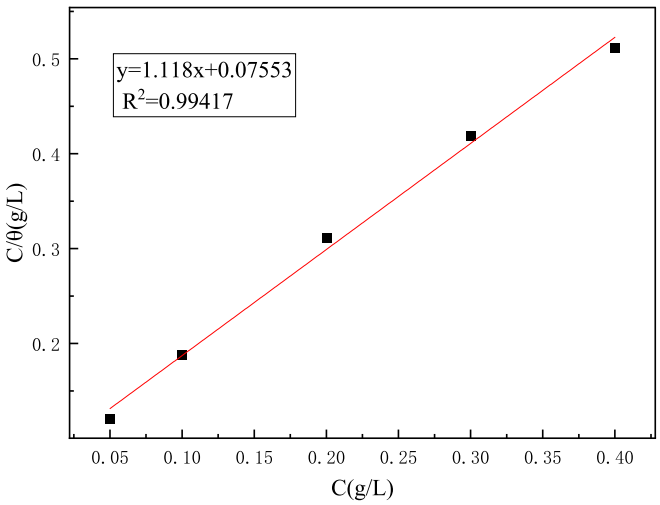

Fig. 15. Langmuir adsorption isotherm of Gly-PESA on Q235 steel surface.

transferring and sharing of electrons between Gly-PESA molecules and empty *d* orbitals of iron atoms formed a complex covalent bond.

3.5.2. *Corrosion inhibition process*

The corrosion inhibition system mainly involved the oxidation of iron atoms in the anode metal and the reduction of oxygen in the cathode. The reactions were as follows (Chen et al., 2019):

$$Fe \rightarrow Fe^{2+} + 2e^{-} \quad (5)$$

$$O_2 + 2H_2O + 4e^{-} \rightarrow 4OH^{-} \quad (6)$$

According to formulas (5) and (6), it could be found that in the blank corrosion system: (i) the dissolution of the steel test piece was accelerated, corrosion products were formed on the surface (such as compounds of Fe^{2+} and Fe^{3+}), and (ii) the reduction reaction of oxygen produced *OH–*, which changed the pH value of the steel surface. When Gly-PESA was added, the corrosion process would be changed. First, due to static electricity, the Gly-PESA molecules were adsorbed on the surface of the steel. The adsorption process could be explained by the displacement reaction of water molecules with Gly-PESA. The substitution reaction equation was as follows (Chen et al., 2019):

$$Gly - PESA_{(so)} + mH_2O_{(ad)} \rightarrow Gly - PESA_{(ad)} + H_2O_{(ad)} \quad (7)$$

where, $Gly\text{-}PESA_{(so)}$ and $Gly\text{-}PESA_{(ad)}$ represented the Gly-PESA molecules in solution and adsorbed on steel surface, respectively, and m represented the number of water molecules replaced by Gly-PESA. Secondly, the chemisorbed process of Gly-PESA occured in the anode region, which could be explained by the combination of the lone electron pair of the heteroatom (oxygen atom) in Gly-PESA with the empty d orbital of the iron atom to form a complex. The reaction in the anode region changed from equation (3) to equation (8):

$$Fe^{2+} + Gly - PESA_{(ad)} \rightarrow [Fe \cdots Gly - PESA]_{ad}^{2+} \quad (8)$$

$[Fe\ldots\ Gly\text{-}PESA]_{(ad)}^{2+}$ represented the complex on the steel surface. It could also be found from equation (8) that when the concentration of Gly-PESA was low, a dense and uniform protective film cannot be formed. Therefore, in practical applications, the dosage of Gly-PESA was increased so that the Gly-PESA molecules combined with iron ions to form enough complexes to protect carbon steel.

Therefore, in the absence of Gly-PESA, the surface of the steel piece was covered with water molecules and a corrosive medium (such as chloride ions and a small amount of oxygen molecules). After the addition of Gly-PESA, its molecules would adsorb on the surface of the steel, separating the carbon steel from the corrosive medium. In addition, due to the many polar groups of Gly-PESA, a dense protective film could be formed on the surface of carbon steel (such as SEM, AFM, XPS analysis), which increased the resistance to erosion, thereby protecting the steel test piece to slow down corrosion.

4. Conclusion

A new scale and corrosion inhibitor (GLY-PESA) was synthesized with PESA and Gly, and characterized by FTIR, ^{1}H NMR and TGA. The scale inhibition efficiency of $CaCO_3$ and $CaSO_4$ was 98.06 % and 92.6 %, respectively and the scale inhibition effect of Gly-PESA was obviously better than that of PESA under the same experimental conditions. SEM, FTIR and XPS experiments showed that Gly-PESA could effectively inhibit the growth of $CaCO_3$ and $CaSO_4$ crystals and cause their crystal lattice distortion or crystal dispersion. As a green corrosion inhibitor, the inhibition efficiency of Gly-PESA on carbon steel reached 78.17 % and the adsorption of Gly-PESA followed Langmuir adsorption isotherm. In addition, through SEM, FTIR, AFM, XPS and CA, it was proved that Gly-PESA formed a protective film on the surface of carbon steel, which increased the corrosion resistance of carbon steel, and effectively protected the surface of the steel. In summary, Gly-PESA was a kind of environment-friendly non-phosphorus scale and corrosion inhibitor, which had good scale and corrosion inhibition performance in industrial circulating cooling water, and broadened the application range of PESA, providing a new idea for the development of industrial scale and corrosion inhibitor.

5. Author agreement

All authors have approved of the publication of this paper. We declare that the paper is the original research.

CRediT authorship contribution statement

Xinhua Liu: Writing – review & editing, Funding acquisition, Formal analysis, Data curation, Conceptualization. **Yuhua Gao:** Writing – original draft, Formal analysis. **Baojing Luo:** Formal analysis. **Hongxia Zhang:** Formal analysis. **Xiaoyu Shi:** Writing – review & editing, Funding acquisition. **Yuan Zhang:** Project administration. **Yongguang Gao:** Investigation. **Ying Wang:** Software. **Zilin Zheng:** Data curation. **Nan Ma:** Data curation. **Jiarui Du:** Funding acquisition. **Linyan Gu:** Data curation.

Declaration of Competing Interest

The authors declare that they have no known competing financial interests or personal relationships that could have appeared to influence the work reported in this paper.

Acknowledgments

This work was financially supported by Natural Science Foundation of Hebei Province of China (D2022105004), the Foundation of Phased Achievement of the Key Cultivation Project of Tangshan Normal University of China (ZDPY07, ZDPY05), Science and Technology Program of Hebei Academy of Sciences of China (No. 24702), and Science and Technology Research Project of Higher Education of Hebei, China (QN2024182).

References

Aah, H.T., Vu, N.S.H., Huyen, L.T., et al., 2020. Ficus racemosa leaf extract for inhibiting steel corrosion in a hydrochloric acid medium. Alex. Eng. J. 59 (6), 4449–4462. https://doi.org/10.1016/j.aej.2020.07.051.

Al-Itawi, H., Al-Mazaideh, G., Al-Rawajfeh, A., et al., 2019. The effect of some green inhibitors on the corrosion rate of Cu, Fe and Al metals. Int. J. Corros. Scale Inhib. 8 (2), 199–211. https://doi.org/10.17675/2305-6894-2019-8-2-3.

Belkheiri, A., Dahmani, K., Mzioud, K., et al., 2024. Advanced evaluation of novel quinoline derivatives for corrosion inhibition of mild steel in acidic environments: A comprehensive electrochemical, computational, and surface study. Int. J. Electrochem. Sci. 19, 100772. https://doi.org/10.1016/j.ijoes.2024.100772.

Chen, J.X., Wang, C., Han, J., et al., 2019. Corrosion inhibition performance of threonine- modified polyaspartic acid for carbon steel in simulated cooling water. J. Appl. Polym. 47242, 1–12. https://doi.org/10.1002/app.47242.

Gu, T.T., Xu, Z.X., Zheng, X.W., et al., 2023. Lycium barbarum leaf extract as biodegradable corrosion inhibitor for copper in sulfuric acid medium. Ind. Crop. Prod. 203, 117181. https://doi.org/10.1016/j.indcrop.2023.117181.

Htet, T.T., Zeng, D.F., 2022. Study on the Corrosion and Scale Inhibition Mechanism of the Thiourea-Modified Polyepoxysuccinic Acid (CNS-PESA). J. Chem. https://doi.org/10.1155/2022/7773199.

Kadhim, A., Al-Amiery, A., Alazawi, R., et al., 2021. Corrosion inhibitors. A review". Int. J. Corros. Scale Inhib. 10 (1), 54–67. https://doi.org/10.17675/2305-6894-2021-10-1-3.

Lai, C., Wang, W., Lv, S.J., et al., 2020. Study on scale and corrosion inhibition performance of ethane-1,2-diaminium-O-O'-dicyclohexyldithiophosphate. Int. J. Electrochem. Sci. 15 (11), 11306–11315. https://doi.org/10.20964/2020.11.05.

Leng, M.X., Lu, X.Y., Feng, W.R., et al., 2020. Study on synthesis and modification of polyepoxysuccinic acid. Frontiers Edu. Res. 3 (6), 30–33. https://doi.org/10.25236/FER.2020.030610.

Liu, X.H., Wang, W.J., Tong, X.J., et al., 2014. Study of corrosion and scale inhibition of polyepoxysuccinic acid derivative. Asian J. Chem. 26 (22), 7716–7720. https://doi.org/10.14233/ajchem.2014.17659.

Liu, X.H., Zhou, K., Han, J., et al., 2018. Scale/corrosion inhibition and biodegradation of lysine modified polyaspartic acid. CIESC J. 69 (5), 2127–2136. https://doi.org/10.11949/j.issn.0438- 1157.20171199.

Liu, X.H., Gao, Y.H., Gao, Y.H., et al., 2023. Synthesis of polyaspartic acid-glycidyl adduct and evaluation of its scale inhibition performance and corrosion inhibition capacity for Q235 steel Applications. Arab. J. Chem. 16, 104515. https://doi.org/10.1016/j.arabjc.2022.104515.

Liu, Z., Li, N., Yan, M.F., et al., 2020. The research progress of water treatment technology on recirculated cooling water. IOP Conf. Ser.: Earth Environ. Sci. 508. https://doi.org/10.1088/1755-1315/508/1/012041.

Mazumder Jafar, M.A., 2020. A review of green scale inhibitors: process, types, mechanism and properties. Coatings 10 (10), 928. https://doi.org/10.3390/coatings10100928.

Meng, Q.W., Chen, D.Z., Yue, L.W., et al., 2007. Hyperbranched polyesters with carboxylic or sulfonic acid functional groups for crystallizationmodification of $CaCO_3$. Macromol. Chem. Phys. 208, 474–484. https://doi.org/10.1002/macp.200600466.

Naka, K., 2003. Effect of dendrimers on the crystallization of $CaCO_3$ in aqueous solution. Top. Curr. Chem. 228, 141–158. https://doi.org/10.1007/b11009.

Nan, Q.L., Li, Q.Q., Zhang, Q.L., et al., 2022. Study of PBBTCA/PESA complex component as a scale inhiitor against calciuum sulfate. Appl. Chem. Ind. 51 (5), 1341–1344. https://doi.org/10.16581/j.cnki.issn1671-3206.20220622.001.

Qiang, Y.J., Guo, L., Li, H., et al., 2021. Fabrication of environmentally friendly Losartan potassium film for corrosion inhibition of mild steel in HCl medium. Chem. Eng. J. 406, 126863. https://doi.org/10.1016/j.cej.2020.126863.

Quraishi, M., Singh, A., Singh, V.K., et al., 2010. Green approach to corrosion inhibition of mild steel in hydrochloric acid and sulphuric acid solutions by the extract of Murraya koenigii leaves. Mater. Chem. Phys. 122 (1), 114–122. https://doi.org/10.1016/j.matchemphys.2010.02.066.

Sharma, S., Kumar, A., 2021. Recent Advances in Metallic Corrosion Inhibition: A Review. J. Mol. Liq. 322, 14862. https://doi.org/10.1016/j.molliq.2020.114862.

Shi, W.Y., Ding, C., Yan, J.L., et al., 2012. Molecular dynamics simulation for interaction of PESA and acrylic copolymers with calcite crystal surfaces. Desalin. 291, 8–14. https://doi.org/10.1016/j.desal.2012.01.019.

Touir, R., Dkhireche, N., Touhami, M.E., et al., 2009. Corrosion and scale processes and their inhibition in simulated cooling water systems by monosaccharides derivatives: Part I: EIS study. Desalin 249 (3), 922–928. https://doi.org/10.1016/j.desal.2009.06.068.

Wan, S., Wei, H.X., Quan, R.X., et al., 2022. Soybean extract firstly used as a green corrosion inhibitor with high efficacy and yield for carbon steel in acidic medium. Ind. Crop Prod. 187, 115354. https://doi.org/10.1016/j.indcrop.2022.115354.

Wang C., Gao B., Zhao P., et al., 2017. Exploration of polyepoxysuccinic acid as a novel draw solution in the forward osmosis process. RSC Adv., 7(49): 30687–30698. https://doi.10.1039/c7ra04036arsc.li/rsc-advances.

Wei, L.J., Lin, Y.H., Li, C.Y., et al., 2022. Performance and mechanism study of PESA-IA as a green oilfield scale inhibitor: experimental and molecular dynamics simulation. J. Polym. Res. 29, 525. https://doi.org/10.1007/s10965-022-03382-y.

Yan, M.F., Tan, Q., Liu, Z., et al., 2020. Synthesis and Application of a Phosphorous-Free and Non-Nitrogen Polymer as an Environmentally Friendly Scale Inhibition and Dispersion Agent in Simulated Cooling Water Systems. ACS Omega 5, 15487–15494. https://doi.org/10.1021/acsomega.0c01620.

Yee, K., Kee, K., Hassas, S., et al., 2019. Corrosion inhibition of molybdate and nitrite for carbon steel corrosion in process cooling water. J. Eng. Sci. Technol. 14 (4), 2431–2444. http://scholars.utp. edu.my/id/eprint/25236.

Zeng, D.F., Qin, W., 2012. Study on a novel composite ecofriendly corrosion and scale inhibitor for steel surface in simulated cooling water. J. Surf. Eng. Mater. Adv. Technol. 2 (3), 137–141. https://doi.org/10.4236/jsemat.2012.23022.

Zhang, K.F., Chen, F.J., Han, J., et al., 2021. Evaluation of Arginine-Modified Polyepoxysuccinic Acid as Anti-scaling and Anti-corrosion Agent. Chem. Eng. Technol., 44 (6), 1131–1140. https://doi.org/10.1002/ceat.202000576.

Zhang, S.P., Qu, H.J., Yang, Z., et al., 2017. Scale inhibition performance and mechanism of sulfamic/amino acids modified polyaspartic acid against calcium sulfate. Desalin. 419, 152–159. https://doi.org/10.1016/j.desal.2017.06.016.

Zhang, B., Zhang, L., Li, F., et al., 2010. Testing the formation of Ca-phosphonate precipitates and evaluating the anionic polymers as Ca-phosphonate precipitates and $CaCO_3$ scale inhibitor in simulated cooling water. Corros. Sci. 52 (12), 3883–3890. https://doi.org/10.1016/j. corsci. 2010.07.037.

Zhang, X.J., Zhao, X.W., Zhang, M.L., et al., 2023. Synthesis, scale inhibition performance evaluation and mechanism study of 3-amino-1-propane sulfonic acid modified polyaspartic acid. Copolym. J. Mol. Struct. 1272, 134141. https://doi.org/10.1016/j.molstruc.2022.134141.

Zhao, H.J., Yang, Y.H., Miao, C.H., et al., 2022. Synthesis and evaluation of amino acid modified polyepoxysuccinic acid as inhibitor of calcium carbonate scale. Water Supply 22 (12), 8923–8941. https://doi.org/10.2166/ws.2022.374.